Temperature dependence of electronic bands in Al/GaN by utilization of invariant deep defect transition energies

Cite as: Appl. Phys. Lett. **119**, 022101 (2021); doi: 10.1063/5.0055409 Submitted: 28 April 2021 · Accepted: 28 June 2021 · Published Online: 12 July 2021







Ji Hyun Kim,^{1,a)} n Pegah Bagheri, n Shun Washiyama, n Andrew Klump, n Ronny Kirste, Seiji Mita, Pramod Reddy, Ramón Collazo, and Zlatko Sitar n

AFFILIATIONS

- Department of Materials Science and Engineering, North Carolina State University, Raleigh, North Carolina 27695, USA
- ²Adroit Materials, Inc., Apex, North Carolina 27539, USA

ABSTRACT

We show experimentally that deep point defect levels in GaN, AlN, and AlGaN are constant with respect to the vacuum level and can be used as invariant internal energy references. This offered a convenient and quick way to assess band shifts and impurity levels as a function of temperature via photoluminescence. For AlGaN, we determined that the band shift in the temperature range of 3–600 K occurred primarily in the valence band and that the lowering of the conduction band edge was comparatively small. The valence band shift (as a fraction of the Varshni bandgap shift) in AlGaN varies from \sim 70% in AlN to \sim 90% in GaN.

Published under an exclusive license by AIP Publishing. https://doi.org/10.1063/5.0055409

AlGaN, with its direct tunable wide bandgap ranging from 3.4 (GaN) to 6.1 eV (AlN) and high breakdown field from 3.75 (GaN) to over 15 MVcm⁻¹ (AlN), has the potential to be exploited for various applications in UV optoelectronics and high-power electronics.¹⁻⁵ However, the development of AlGaN-based technology faces significant challenges due to compensating defects⁶ and large threading dislocation density (TDD) arising from a large lattice mismatch with the typically employed foreign substrates.⁷⁻¹⁰ Furthermore, the challenges increase for Al-rich AlGaN with relatively poor Ohmic contacts and high dopant ionization energies due to the possible DX formation.^{8,11–13} While utilization of native substrates, such as single crystal AlN or GaN, reduces the TDD to <10³ cm⁻² from typical values of 10⁹ cm⁻² on sapphire, ^{14,15} compensating point defects still present a challenge for further development of AlGaN-based technology, 6,16-20 requiring an understanding of the nature of the defects and the dependence of their formation on the growth and processing environment. While various defect states or electronic bands are well-researched in the binary alloys, AlGaN as a ternary alloy does not share the same wealth of knowledge. 13,21,22 Additionally, understanding point defect formation at relevant temperatures, beyond the typical 0 K equilibrium models, is of technological importance. Being able to easily identify compensating defect configurations or nonradiative centers for relevant compositions and temperatures would aid improving devices.

Previously, the energy levels of the conduction band minimum and the valence band maximum for AlGaN have been estimated with respect to the reference vacuum level as a function of Al composition via XPS.²⁵ Furthermore, the charge neutrality level at the surface (i.e., the surface Fermi level pinning) was also determined with respect to the vacuum level and was found to be independent of alloy composition, indicating a surface work function independent of alloy composition.²⁴ In addition to these, it was observed that point defects that form localized deep states within the bandgap are at a constant energy with respect to the vacuum level and are also independent of the alloy composition.²⁶ This was in agreement with the universality rule predicting the independent nature of the deep mid-gap states for both cationic and anionic impurities.²⁶⁻²⁹ Therefore, this suggested that the point defect thermodynamic transition energies and the charge neutrality level could be readily utilized as reference energies. Although deep defects are internal reference states that remain invariant with respect to the vacuum level as a function of composition and temperature, 26 they are still expected to undergo thermal broadening due to lattice interactions.³⁰ This invariance of the deep levels offers a convenient internal reference as the energy transitions between the defect states and the electronic bands can simply be determined by luminescence.

In this work, we utilize localized energy states associated with deep defects as an internal absolute reference to determine the shift of

^{a)}Author to whom correspondence should be addressed: jkim69@ncsu.edu

electronic bands in AlGaN as a function of temperature. We confirm the relative invariance of thermodynamic transition levels of deep defects with changes in electron-lattice interactions by studying the temperature dependence of the Stokes shift. As further validation of the temperature invariance hypothesis of the deep defect states, in general, we demonstrate that the measured electronic band shifts are independent of the identity of the localized deep defect. This approach may be crucial not only for obtaining accurate point defect configurations in Al/GaN with respect to composition and temperature but also for estimating dopant thermodynamics as a function of growth temperature.

All of the samples included in this work were grown on AlN single crystal substrates or AlN templates on c-plane sapphire substrates via low pressure metal organic chemical vapor deposition (MOCVD). The details on the AlN crystal growth by physical vapor transport, growth of AlN templates on sapphire, and pre-epitaxy AlN surface preparation are described elsewhere. AlGaN layers were grown between 950 and 1150 °C, depending on the Al composition, under a constant total reactor pressure of 20 Torr, using Trimethylaluminum (TMA), Triethylgallium (TEG), and NH3 as Al, Ga, and N precursors, respectively.

For the PL measurements, a 193 nm ArF excimer laser was used as an excitation light source (a 50 ns pulse width and a repetition rate of 100 Hz). The power density of the laser was kept low as not to influence the temperature of the sample on a stage with a cooling capacity of 1.5 W at 4.2 K. The luminescence from the samples was dispersed in a 0.75 m Acton Series SP-2750 monochromator with a 150 grooves/mm diffraction grating and detected by a PIXIS 2 K charge-coupled device (CCD) camera. The higher temperature setup utilized a UV-transparent optical fiber attachment (Princeton Instruments SP2750) that could be placed closer to the sample. For low temperature PL (3–300 K), the samples were placed inside a Janis (SHI-RDK-415D) closed-cycle helium cryostat, while for high temperatures (300–600 K), a metal-ceramic heater (THORLABS HT24S) was used.

Since C_N is a commonly observed and studied deep point defect in AlGaN, its thermodynamic transition energy, $C_N^{-1} - C_N 0$, was chosen as an internal reference. $^{35-37,39}$ The C_N -based results were corroborated with V_{III}+nSi as an additional invariant deep point defect. The dominant point defect was chosen either as C_N or V_{III}+nSi, and their formation or incorporation was accordingly controlled employing chemical potential control and is described elsewhere. 38,39 The band diagram was constructed using the data obtained from the temperature dependent PL. The invariant deep point defect was placed at a reference point of 0. Then, the relative position of the conduction band with respect to a chosen deep level thermodynamic transition (C_N) was determined, using the energy of the corresponding luminescence peak corrected for the Stokes shift, which was measured as a difference between the absorption and emission peaks. With the known position of the conduction band, the position of the valence band was determined from the near-band edge (NBE) luminescence. Hence, the band diagram could be constructed over the whole characterized temperature range of 3-600 K.

In addition to the invariance of the deep level, this method requires that the change in the Stokes shift with temperature is small compared to the change in the bandgap energy, which seems to hold true, in general, for III-nitrides. Several authors have demonstrated experimentally that the Stokes shift for various InGaN compositions

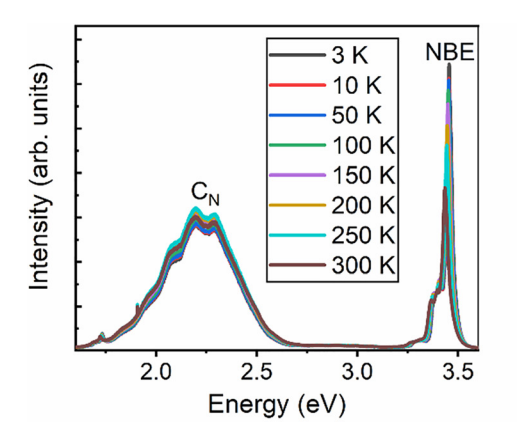
was independent of temperature. $^{40-42}$ The insignificance of thermal effects on the Stokes shift was also confirmed for AlN by PL (\sim 3.9 eV) and absorption measurements (\sim 4.7 eV). The energy difference between the luminescence and the absorption band (Stokes shift) was measured to remain virtually constant with temperature at 0.8 eV. 43 The error in the luminescence peak fit was around $10\,\text{meV}$, and thus, the change in the Stokes shift was negligible compared to the change in the bandgap of about $60\,\text{meV}$ over the same temperature range.

The PL spectra of GaN, Fig. 1, from 3 to 600 K illustrate the expected Varshni relationship. Notably, the near band edge emission (NBE) (3.4 eV at RT) shifts significantly more for high temperature excursions (200 meV for $300\,\mathrm{K} \to 600\,\mathrm{K}$) than for the low ones (20 meV for 300 K \rightarrow 3 K). ^{2,44} It is important to note that the shift of the C_N emission peak (2.2 eV at RT) is negligible compared to that of the shift of the NBE for low and high temperature regimes. This is most notable in the high temperature PL spectra, which show a 200 meV shift in the NBE emission and no discernable shift in the carbon-related emission (Fig. 1, right). Similar trends were observed in Al_{0.4}Ga_{0.6}N and AlN, where the position of the C_N peak remains relatively constant at 2.7 and 3.9 eV, respectively, while the position of the NBE changes significantly. It should be noted that the PL intensity decreased at higher temperatures. The observed thermal quenching of defects is dependent on an activation energy resulting in a decrease beyond a certain thermal energy and differs from that of the NBE. 45 Since we are employing the defect peak as a reference, the reduction in intensity at higher temperatures may provide a (defect dependent) high temperature limit for studying the band dependence on temperature. The PL presented did not reach this limit at the highest temperatures of 600 K.

Temperature-dependent band diagrams for GaN and AlN were constructed from the PL data as described above and are shown in Fig. 2. It is noted that the change in the bandgap with temperature (Varshni shift) seems to be dominated by the raise in the valence band energy. The ratio of the change in the conduction band to the valence band in GaN was measured to be \sim 1:10, while that in AlN was \sim 1:2.5.

The relative changes in the conduction and valence bands can be derived from the second order perturbation theory, where the perturbation is associated with the change in the Hamiltonian due to various contributions from an increase in temperature, as predicted by Mahan for the bandgap dependence in CdTe. 46 The main conclusion of this analysis was that the change in the energy for each band was roughly proportional to the respective effective masses. Mahan also finds the negligible temperature dependence of the conduction band in CdTe due to its small electron effective mass, while the valence band showed larger temperature dependence due to a larger effective mass of the holes and a stronger interaction with acoustic phonons. 46 The effective masses of the holes in GaN and AlN are 1.5 m₀ and 3.5 m₀, respectively, 47,48 while the effective masses of electrons are 0.2 m₀ and 0.4 m₀, respectively. 44,49 Consequently, the valence band is expected to experience a greater thermal shift than the conduction band, as observed experimentally. Note that the quoted hole effective masses are for heavy holes only, so the comparison of effective masses yields only qualitative results while the experimental results are quantitative.

Finally, we characterized AlGaN at two different compositions: $Al_{0.4}Ga_{0.6}N$ and $Al_{0.4}Ga_{0.6}N$. As further validation of our hypothesis



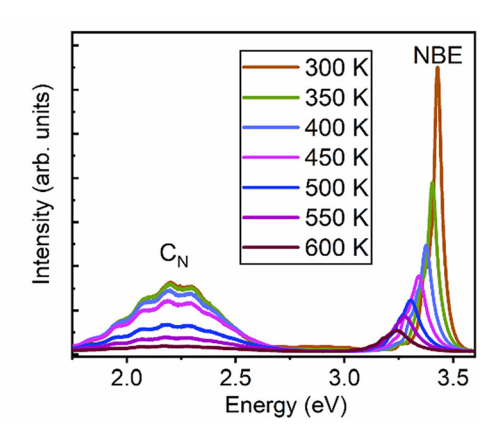


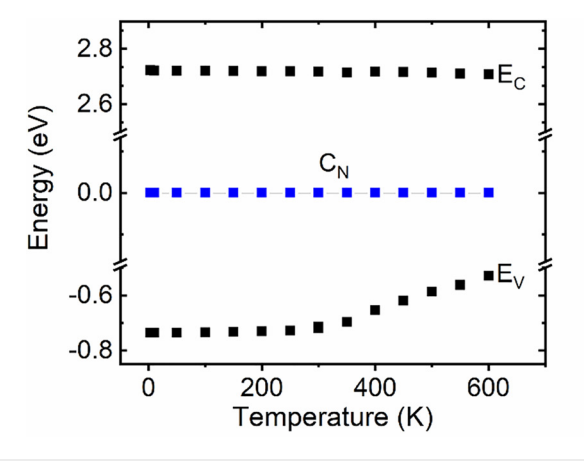
FIG. 1. (left) Low (3–300 K) and (right) high temperature (300–600 K) PL of GaN showing the near-band edge (NBE) and C_N peaks. While there was a significant red shift of the NBE with temperature, the position of the C_N peak remained practically constant over the whole temperature range.

that the deep defects are practically invariant with temperature, we also demonstrate that the electronic band shifts with temperature determined by this method are independent of the identity of the localized deep defect. Hence, we employ the $V_{\rm III}+n\rm Si$ as the second deep-defect in addition to $C_{\rm N}$ to validate our hypothesis and corroborate the measured band shifts as seen by the PL in Fig. 3 for $\rm Al_{0.4}\rm Ga_{0.6}\rm N$. The observations seen for the band shifts in $\rm Al_{0.4}\rm Ga_{0.6}\rm N$, with $\rm V_{\rm III}$ related complex, as seen from Fig. 4 (right) can be directly compared to Fig. 4 (left), where $\rm C_{\rm N}$ emission energy is used as the reference energy. The band shifts of the conduction and valence bands in $\rm Al_{0.4}\rm Ga_{0.6}\rm N$ and $\rm Al_{0.6}\rm Ga_{0.4}\rm N$ (Fig. 5) measured with $\rm C_{\rm N}$ and $\rm V_{\rm III}$ -complex yield similar values at ~ 1.4 , supporting our reference energy hypothesis and indicating the valence band shift for AlGaN lies between the $\sim 90\%$ in GaN and $\sim 70\%$ in AlN.

This provides an interesting insight into the band shift with respect to temperature and the defect configurations that follow. For example, due to the predominant valence band shift with temperature in GaN, for an acceptor type defect with a (0/-1) transition, such as Mg, the ionization energy is expected to decrease with temperature, and the decrease should be approximately equal to the decrease in the

bandgap. Similarly, due to the conduction band being almost constant with T, the Schottky barrier (determined by the defects pinning the surface Fermi level) is expected to be practically constant with temperature in the n-type material but should decrease with temperature for the p-type material. Finally, the acceptor-type impurities may show a stronger growth temperature dependence, while donor type impurities are expected to be fairly independent of the growth temperature. Similar predictions have been described by Zunger, where shallow impurities track closely the host band-edges with the shift of the bands.²⁷

Using deep impurity levels as an internal reference (C_N and $V_{III}+nSi$), we used PL to measure the shift of the electronic bands as a function of temperature for GaN, $Al_{0.4}Ga_{0.6}N$, and AlN. In contrast to the previously predicted and observed band shifts, where the valence band shift was estimated to be $\sim 70\%$ of the Varshni shift, we observed for the temperature range of 3–600 K that the shift was predominantly in the valence band, and it amounted to $\sim 70\%$ and $\sim 90\%$ of the total shift for AlN and GaN, respectively. Utilizing a deep point defect as an invariant internal reference, as opposed to the vacuum level that cannot be easily measured, offers a convenient way to assess band shifts



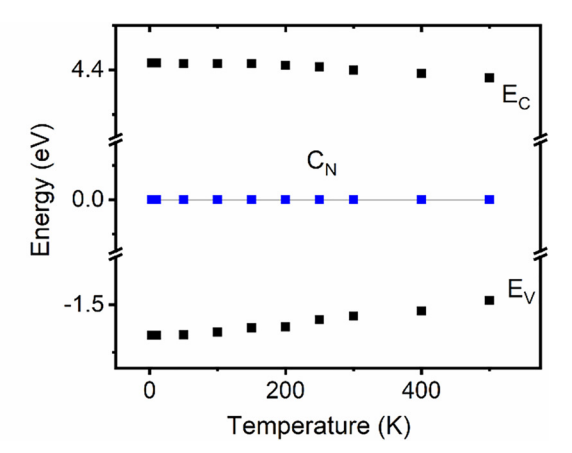
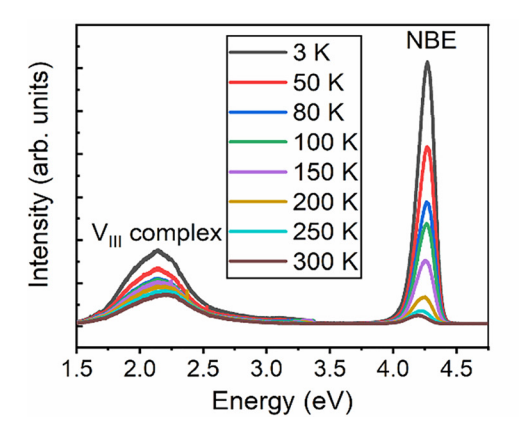


FIG. 2. Temperature-dependent band diagrams for (left) GaN and (right) AIN. In both cases, the conduction band remained relatively constant with temperature while most of the change was in the valence band.



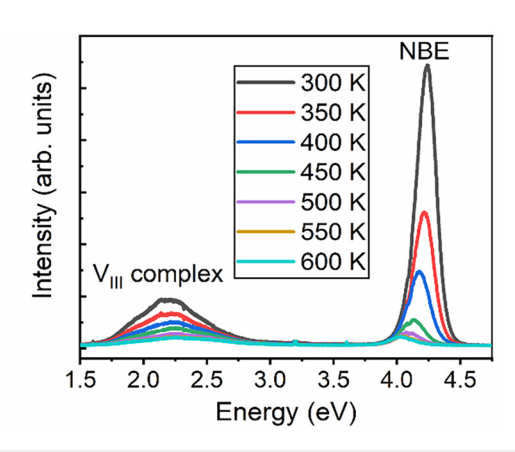
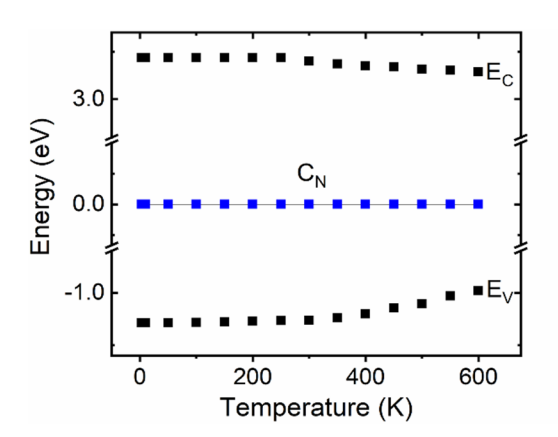


FIG. 3. (left) Low (3–300 K) and (right) high temperature (300–600 K) PL of AlGaN showing V_{III}-complex and NBE peaks. Note the temperature invariance of the V_{III}-complex.



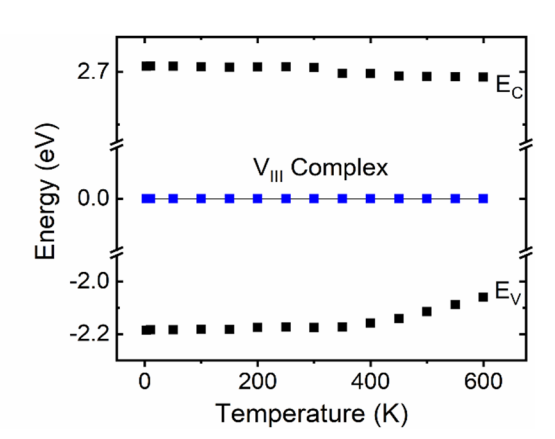


FIG. 4. Temperature-dependent band diagram of $Al_{0.4}Ga_{0.6}N$ constructed using (left) C_N and (right) V_{III} -complex as a reference. The different relative energy scales for (left) and (right) arise from the fact that the two defects have different energy levels but are here both referenced to 0 eV. Note that this has no influence on the shift of the bands.

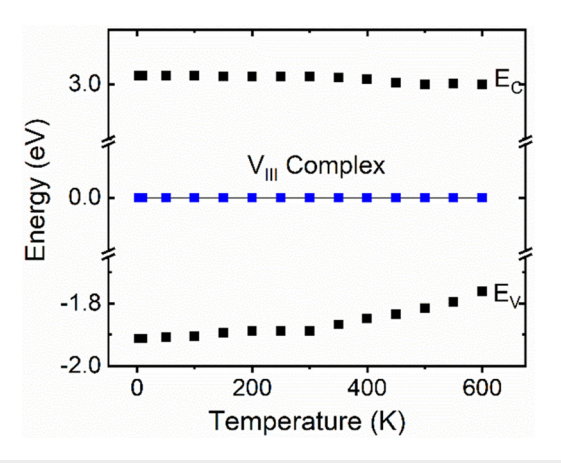


FIG. 5. Temperature-dependent band diagram of $AI_{0.6}Ga_{0.4}N$ constructed using V_{III} -complex as a reference.

and impurity levels as a function of temperature. In addition, these results prove to be pertinent to estimates of dopant incorporation at growth temperatures.

The authors acknowledge funding in part from AFOSR (Nos. FA9550-17-1-0225, FA9550-19-1-0114, and FA9550-19-1-0358), NSF (Nos. ECCS-1508854, ECCS-1916800, and ECCS-1653383), and ARO (No. W911NF-16-C-0101).

DATA AVAILABILITY

The data that support the findings of this study are available within the article.

REFERENCES

¹Z. Bryan, I. Bryan, J. Xie, S. Mita, Z. Sitar, and R. Collazo, Appl. Phys. Lett. **106**, 142107 (2015).

²Y. P. Varshni, *Physica* **34**, 149 (1967).

³H. Ohta, N. Kaneda, F. Horikiri, Y. Narita, T. Yoshida, T. Mishima, and T. Nakamura, IEEE Electron Device Lett. **36**, 1180 (2015).

- ⁴J. Y. Tsao, S. Chowdhury, M. A. Hollis, D. Jena, N. M. Johnson, K. A. Jones, R. J. Kaplar, S. Rajan, C. G. V. de Walle, E. Bellotti, C. L. Chua, R. Collazo, M. E. Coltrin, J. A. Cooper, K. R. Evans, S. Graham, T. A. Grotjohn, E. R. Heller, M. Higashiwaki, M. S. Islam, P. W. Juodawlkis, M. A. Khan, A. D. Koehler, J. H. Leach, U. K. Mishra, R. J. Nemanich, R. C. N. Pilawa-Podgurski, J. B. Shealy, Z. Sitar, M. J. Tadjer, A. F. Witulski, M. Wraback, and J. A. Simmons, Adv. Electron. Mater. 4, 1600501 (2018).
- ⁵M. Shur, Solid-State Electron. 155, 65 (2019).
- ⁶P. Reddy, M. P. Hoffmann, F. Kaess, Z. Bryan, I. Bryan, M. Bobea, A. Klump, J. Tweedie, R. Kirste, S. Mita, M. Gerhold, R. Collazo, and Z. Sitar, J. Appl. Phys. 120, 185704 (2016).
- ⁷P. Cantu, F. Wu, P. Waltereit, S. Keller, A. E. Romanov, U. K. Mishra, S. P. DenBaars, and J. S. Speck, Appl. Phys. Lett. **83**, 674 (2003).
- ⁸I. Bryan, Z. Bryan, S. Washiyama, P. Reddy, B. Gaddy, B. Sarkar, M. H. Breckenridge, Q. Guo, M. Bobea, J. Tweedie, S. Mita, D. Irving, R. Collazo, and Z. Sitar, Appl. Phys. Lett. **112**, 062102 (2018).
- ⁹B. E. Gaddy, Z. Bryan, I. Bryan, R. Kirste, J. Xie, R. Dalmau, B. Moody, Y. Kumagai, T. Nagashima, Y. Kubota, T. Kinoshita, A. Koukitu, Z. Sitar, R. Collazo, and D. L. Irving, Appl. Phys. Lett. 103, 161901 (2013).
- ¹⁰J. S. Harris, J. N. Baker, B. E. Gaddy, I. Bryan, Z. Bryan, K. J. Mirrielees, P. Reddy, R. Collazo, Z. Sitar, and D. L. Irving, Appl. Phys. Lett. 112, 152101 (2018).
- ¹¹P. Bagheri, R. Kirste, P. Reddy, S. Washiyama, S. Mita, B. Sarkar, R. Collazo, and Z. Sitar, Appl. Phys. Lett. 116, 222102 (2020).
- ¹²M. D. McCluskey, C. G. Van de Walle, N. M. Johnson, D. P. Bour, and M. Kneissl, Int. J. Mod. Phys. B 13, 1363 (1999).
- ¹³L. Gordon, J. L. Lyons, A. Janotti, and C. G. Van de Walle, Phys. Rev. B 89, 085204 (2014).
- ¹⁴Z. G. Herro, D. Zhuang, R. Schlesser, R. Collazo, and Z. Sitar, J. Cryst. Growth 286, 205 (2006).
- ¹⁵ A. Rice, R. Collazo, J. Tweedie, R. Dalmau, S. Mita, J. Xie, and Z. Sitar, J. Appl. Phys. **108**, 043510 (2010).
- ¹⁶Z. Bryan, I. Bryan, B. E. Gaddy, P. Reddy, L. Hussey, M. Bobea, W. Guo, M. Hoffmann, R. Kirste, J. Tweedie, M. Gerhold, D. L. Irving, Z. Sitar, and R. Collazo, Appl. Phys. Lett. 105, 222101 (2014).
- ¹⁷S. F. Chichibu, A. Uedono, K. Kojima, H. Ikeda, K. Fujito, S. Takashima, M. Edo, K. Ueno, and S. Ishibashi, J. Appl. Phys. 123, 161413 (2018).
- ¹⁸D. Monti, M. Meneghini, C. De Santi, G. Meneghesso, E. Zanoni, J. Glaab, J. Rass, S. Einfeldt, F. Mehnke, J. Enslin, T. Wernicke, and M. Kneissl, IEEE Trans. Electron Devices 64, 200 (2017).
- ¹⁹A. Uedono, S. Ishibashi, K. Tenjinbayashi, T. Tsutsui, K. Nakahara, D. Takamizu, and S. F. Chichibu, J. Appl. Phys. 111, 014508 (2012).
- ²⁰H. Amano, R. Collazo, C. D. Santi, S. Einfeldt, M. Funato, J. Glaab, S. Hagedorn, A. Hirano, H. Hirayama, R. Ishii, Y. Kashima, Y. Kawakami, R. Kirste, M. Kneissl, R. Martin, F. Mehnke, M. Meneghini, A. Ougazzaden, P. J. Parbrook, S. Rajan, P. Reddy, F. Römer, J. Ruschel, B. Sarkar, F. Scholz, L. J. Schowalter, P. Shields, Z. Sitar, L. Sulmoni, T. Wang, T. Wernicke, M. Weyers, B. Witzigmann, Y.-R. Wu, T. Wunderer, and Y. Zhang, J. Phys. D: Appl. Phys. 53, 503001 (2020).
- ²¹M. A. Reshchikov, J. Appl. Phys. **127**, 055701 (2020).
- ²²P. Kempisty, Y. Kangawa, A. Kusaba, K. Shiraishi, S. Krukowski, M. Bockowski, K. Kakimoto, and H. Amano, Appl. Phys. Lett. 111, 141602 (2017).
- ²³Z. Ma, A. Almalki, X. Yang, X. Wu, X. Xi, J. Li, S. Lin, X. Li, S. Alotaibi, M. Al huwayz, M. Henini, and L. Zhao, J. Alloys Compd. 845, 156177 (2020).

- ²⁴A. Armstrong, A. A. Allerman, T. A. Henry, and M. H. Crawford, Appl. Phys. Lett. 98, 162110 (2011).
- ²⁵P. Reddy, I. Bryan, Z. Bryan, J. Tweedie, S. Washiyama, R. Kirste, S. Mita, R. Collazo, and Z. Sitar, Appl. Phys. Lett. 107, 091603 (2015).
- ²⁶P. Reddy, Z. Bryan, I. Bryan, J. H. Kim, S. Washiyama, R. Kirste, S. Mita, J. Tweedie, D. L. Irving, Z. Sitar, and R. Collazo, Appl. Phys. Lett. 116, 032102 (2020).
- ²⁷A. Zunger, Phys. Rev. Lett. **54**, 849 (1985).
- ²⁸M. J. Caldas, A. Fazzio, and A. Zunger, Appl. Phys. Lett. **45**, 671 (1984).
- ²⁹J. L. Lyons, A. Janotti, and C. G. Van de Walle, J. Appl. Phys. 115, 012014 (2014).
- ³⁰A. Owens, Semiconductor Radiation Detectors (CRC Press, 2019).
- ³¹P. Lu, R. Collazo, R. F. Dalmau, G. Durkaya, N. Dietz, B. Raghothamachar, M. Dudley, and Z. Sitar, J. Cryst. Growth 312, 58 (2009).
- ³²S. Washiyama, Y. Guan, S. Mita, R. Collazo, and Z. Sitar, J. Appl. Phys. 127, 115301 (2020).
- ³³H. Miyake, G. Nishio, S. Suzuki, K. Hiramatsu, H. Fukuyama, J. Kaur, and N. Kuwano, Appl. Phys. Express 9, 025501 (2016).
- ³⁴H. Fukuyama, H. Miyake, G. Nishio, S. Suzuki, and K. Hiramatsu, Jpn. J. Appl. Phys., Part 1 55, 05FL02 (2016).
- 35M. A. Reshchikov, N. M. Albarakati, M. Monavarian, V. Avrutin, and H. Morkoç, J. Appl. Phys. 123, 161520 (2018).
- 36J. L. Lyons, A. Janotti, and C. G. V. de Walle, Appl. Phys. Lett. 97, 152108 (2010).
- ³⁷R. Collazo, J. Xie, B. E. Gaddy, Z. Bryan, R. Kirste, M. Hoffmann, R. Dalmau, B. Moody, Y. Kumagai, T. Nagashima, Y. Kubota, T. Kinoshita, A. Koukitu, D. L. Irving, and Z. Sitar, Appl. Phys. Lett. 100, 191914 (2012).
- ⁵⁸P. Reddy, S. Washiyama, F. Kaess, R. Kirste, S. Mita, R. Collazo, and Z. Sitar, J. Appl. Phys. **122**, 245702 (2017).
- ³⁹S. Washiyama, P. Reddy, B. Sarkar, M. H. Breckenridge, Q. Guo, P. Bagheri, A. Klump, R. Kirste, J. Tweedie, S. Mita, Z. Sitar, and R. Collazo, J. Appl. Phys. 127, 105702 (2020).
- ⁴⁰H. Kudo, K. Murakami, H. Ishibashi, R. Zheng, Y. Yamada, and T. Taguchi, Phys. Status Solidi B 228, 55 (2001).
- ⁴¹D. R. Hang, M. M. C. Chou, M. H. Hsieh, and M. Heuken, J. Korean Phys. Soc. 53, 1584 (2008).
- ⁴²C. Sasaki, H. Naito, M. Iwata, H. Kudo, Y. Yamada, T. Taguchi, T. Jyouichi, H. Okagawa, K. Tadatomo, and H. Tanaka, J. Appl. Phys. 93, 1642 (2003).
- 43D. Alden, J. S. Harris, Z. Bryan, J. N. Baker, P. Reddy, S. Mita, G. Callsen, A. Hoffmann, D. L. Irving, R. Collazo, and Z. Sitar, Phys. Rev. Appl. 9, 054036
- 44V. Bougrov, M. E. Levinshteĭn, S. L. Rumyantsev, and A. Zubrilov, Properties of Advanced Semiconductor Materials: GaN, AlN, InN, BN, SiC, SiGe (Wiley, New York, 2001), p. 4.
- 45V. Pagonis, C. Ankjærgaard, A. S. Murray, M. Jain, R. Chen, J. Lawless, and S. Greilich, J. Lumin. 130, 902 (2010).
- 46 G. D. Mahan, J. Phys. Chem. Solids 26, 751 (1965).
- ⁴⁷M. Leszczynski, H. Teisseyre, T. Suski, I. Grzegory, M. Bockowski, J. Jun, S. Porowski, K. Pakula, J. M. Baranowski, C. T. Foxon, and T. S. Cheng, Appl. Phys. Lett. 69, 73 (1996).
- 48M. Suzuki and T. Uenoyama, J. Appl. Phys. 80, 6868 (1996).
- 49Y.-N. Xu and W. Y. Ching, Phys. Rev. B 48, 4335 (1993).